Texture contrast: Ultrasonic characterization of stacked gels' deformation during compression on a biomimicking tongue

Rohit Srivastava, Markus Stieger, Elke Scholten, Isabelle Souchon, Vincent Mathieu

Current Research in Food Science 4 (2021) 449–459

Contents lists available at ScienceDirect

Current Research in Food Science

journal homepage: www.sciencedirect.com/journal/current-research-in-food-science

Texture contrast: Ultrasonic characterization of stacked gels' deformation during compression on a biomimicking tongue☆

Rohit Srivastava [a], Markus Stieger [b], Elke Scholten [c], Isabelle Souchon [d], Vincent Mathieu [a,*]

[a] Université Paris-Saclay, INRAE, AgroParisTech, UMR SayFood, F-78850, Thiverval-Grignon, France
[b] Division of Human Nutrition and Health & Food Quality and Design, Wageningen University, PO Box 17 6700 AA Wageningen, the Netherlands
[c] Physics and Physical Chemistry of Foods, Wageningen University, PO Box 17 6700 AA Wageningen, the Netherlands
[d] UMR 408 SQPOV, INRAE, Avignon Université, F-84000 Avignon, France

ARTICLE INFO

Handling Editor. NO

Keywords:
Food texture
Oral processing
Ultrasound
Artificial tongue models
Composite food gels

ABSTRACT

When undergoing compression during oral processing, stacked gels display different mechanical properties that shape perceptions of texture contrasts (Santagiuliana et al., 2018). However, to date, characterizing the mechanical responses of individual gel layers has been impossible. In this study, an ultrasound (US) technique was developed, that allowed such deformation dynamics to be visualized in real time. Stacked gels were created using layers (height: 5 mm) of brittle agar and elastic gelatin in different combinations. In a series of experimental tests, different stacked gel combinations were placed on a rough, deformable artificial tongue model (ATM) made of polyvinyl alcohol; a texture analyzer was used to apply uniaxial force, and deformation was monitored by an US transducer (5 MHz) located under the ATM.

From the obtained results, it was observed that the deformation of ATM surface during compression was in accordance with the force recorded by the texture analyzer, suggesting a collaborative response of different layers under compression. Moreover, US imaging revealed that differences in Young's modulus values between layers led to heterogeneous strain distributions, which were more pronounced for the agar layers. Biopolymer elasticity was also a key factor. Regardless of combination type, the gelatin layers never fractured; such was not the case for the agar layers, especially those with lower Young's modulus values. The results of this US study have thus paved the way for a better understanding of the mechanical deformation that occurs in heterogeneous foods, a phenomenon that has been difficult to examine because of the limitations of conventional techniques.

1. Introduction

The solid and liquid foods that make up our diets have diverse structures and mechanical properties. Some have rather homogeneous structures. In recent years, homogeneous foods have been prominently used to clarify how they are processed in the mouth and how texture perceptions arise as a result. Studies have been carried out on actual foods, including breads, cookies, cheeses, and custards, to characterize food mechanical properties during oral processing (De Wijk et al., 2006a; Le Bleis, Chaunier, Della Valle, Panouillé and Réguerre, 2013; Saint-Eve et al., 2015; Young et al., 2013). However, such foods only represent a small portion of our diets. Indeed, most foods are more complex; they are heterogeneous composites, combining different phases with highly contrasting mechanical properties. Altering such properties when formulating foods impacts the sensory experience of the consumer (Palczak et al., 2020; Szczesniak and Kahn, 1984). Customizing food properties can also serve as a tool for improving nutritional quality (e.g., reduction of sugar, salt, and fat content or changes in digestive and nutrient-release kinetics) (Mesurolle et al., 2013; Salles et al., 2017; Singh et al., 2015). In recent years, interest has grown in creating model foods that display different levels of structural heterogeneity as a mean for understanding the phenomena behind the perception of texture contrasts (Devezeaux de Lavergne et al., 2016; Laguna and Sarkar, 2016; Larsen et al., 2016; Santagiuliana, Piqueras-Fiszman, van der Linden, Stieger and Scholten, 2018; Santagiuliana et al., 2019). In homogeneous foods, macroscopic textural

☆ Submitted to: **Current Research in Food Science**.

* Corresponding author. Paris-Saclay Food and Bio-product Engineering Laboratory (SayFood UMR 782) Joint Research Unit INRAE AgroParisTech Bâtiment CBAI 1, avenue Lucien Brétignières 78850 Thiverval-Grignon, France.
E-mail address: vincent.mathieu@inrae.fr (V. Mathieu).

https://doi.org/10.1016/j.crfs.2021.06.004
Received 21 April 2021; Received in revised form 24 June 2021; Accepted 24 June 2021
Available online 3 July 2021

properties can be rather easily verified and assessed. In contrast, in composite foods, the presence of structural heterogeneity presents a challenge: it is harder to predict texture perceptions because different structures have different mechanical properties. The individual structural components of a composite food may interact and deform synergistically during oral processing, making it difficult to trace the drivers of texture perception dynamics.

Devezeaux de Lavergne et al. (2016) studied how mechanical contrasts in stacked gels (two layers of emulsion-filled agar/gelatin gels with mechanical contrast) affected oral processing and texture perception dynamics, as measured via a sensory panel. Their results showed that, overall texture perception dynamics of the combined layers was the average of that of two individual layers. However, these interesting findings were difficult to interpret from a mechanical perspective because the layers' mechanical characteristics were quantified separately using a texture analyzer with a cylindrical probe.

Going a step further, Santagiuliana et al. (2018) used stacked gels (two layers) to investigate how the mechanical and physicochemical properties of individual gel layers influenced perceived heterogeneity. Here, interestingly, the mechanical characteristics of the stacked gels were directly measured using a penetration test that employed a texture analyzer with a wedge probe. Consequently, it was observed that the fracture force of the top layer had an impact on that of the bottom layer. The same study also investigated how differences in fracture stress between two layers affected the perception of texture contrasts. One of the main conclusions was that, depending on polymer type, a minimum degree of difference (5 kPa for soft and brittle agar layers; 16 kPa for soft and elastic gelatin layers) in fracture stress between the two layers was required for heterogeneity to be perceived. Taken together, these discoveries greatly clarified the bulk deformation dynamics that occur between different layers and the synergistic effects on the deformation kinetics of the entire system. It is thus evident that the distribution of stress/strain in each layer must be characterized during compression. To identify the layers' individual contributions, it is not enough to assess the system's overall mechanical properties using uniaxial compression tests; a complimentary approach is needed, in which real oral conditions, such as soft contacts between the palate and tongue, are mimicked.

Kohyama et al. (2019) presented an innovative approach of compressing soft food gels between an artificial tongue (transparent urethane gels) and plate, and monitored the deformation incurred by the gels with the help of video cameras. This approach was found very effective in analyzing the deformation and fracture phenomena in monolayer gels. However, they can pose some technical difficulties when several interfaces are stacked over each other. Depending on the color contrast between the media, or the level differences between the camera axis and the different interfaces, there may be some errors in the estimation of the deformations.

To overcome these limitations, ultrasonic methods can be a good candidate. Ultrasound based techniques being non-invasive and non-destructive, they have gained interest by the community of food science for the real-time and quantitative monitoring of various physical phenomena occurring during food processing (De Wijk et al., 2006b). Indeed, ultrasonic waves are mechanical waves, sensitive to the mechanical properties of the media and interfaces in which they propagate. In addition to the well-known imaging approaches that allow to explore qualitatively the heterogeneities in the media, they can be used quantitatively to characterize properties (propagation speed, attenuation, acoustic impedance) revealing the mechanical characteristics of the propagation media. Two recent studies (Mantelet et al., 2020a,b) described a method in which real-time quantitative ultrasound was used to explore coupling phenomena between food gels (agar and gelatin) and tongue-mimicking surfaces. Moreover in our recent study (Srivastava et al., 2021), a quantitative ultrasound method has been proposed to quantify the deformation dynamics of artificial tongue models during the compression of monolayer gels. The characterization of the tongue deformation was achieved by the use of single element transducers. Unlike multi-element imaging probes, the measurement of deformations with mono-element transducers does not face limitations induced by image resolution. Thanks to signal processing methods, they allowed an accurate estimation of the tongue deformation, by the measurement of changes in the time of flight (ToF) of ultrasound echoes reflecting back from the tongue-food interface. This type of mono-element transducer thus allows a precise quantification of the deformations in the direction corresponding to the beam axis. However, they only reflect what happens in the core of the samples (with variable beam sizes, but generally several millimeters in diameter), and they are thus not as suitable as multi element array probes for quantifying gradients of deformation along the direction perpendicular to the beam (from the core to the periphery of the interfaces).

Against this backdrop, the aim of the study presented here was twofold. First, it sought to build upon previous research by determining whether a quantitative ultrasound method could characterize not only the deformation of an artificial tongue, but also that of a heterogeneous food, modelled using stacked gels. Second, it explored how the deformation dynamics of the system and its components were influenced by (i) associations between gel layers; (ii) differences in mechanical properties between the two layers; and (iii) layer position on the artificial tongue. Drawing upon the work of Santagiuliana et al. (2018), agar and gelatin gels of differing concentrations (which thus displayed different mechanical properties) were created and combined to form stacked gels consisting of two layers. Then, the gels were placed on a deformable artificial tongue model (ATM), and the entire system underwent uniaxial compression induced by a hard, flat probe that mimicked the palate (Fig. 1a). Ultrasound pulse-echo approaches and associated signal processing methods were developed to monitor the deformation dynamics of the different system components during the compression test.

2. Materials and methods

2.1. Preparation of the stacked gels

Two types of polymers were used in this study: agar (Ag) and gelatin (Ge). Gel composition and preparation protocols were similar to those in Santagiuliana et al. (2018). Each gel layer was identified using a polymer abbreviation (Ag and Ge) followed by a number corresponding to the gel's fracture stress (kPa). The solutions of agar (HP700IFG, Kalys, Bernin, France) and gelatin (Bloom 250 PS 8/3 Rousselot, Gent, Belgium) were prepared using demineralized water and then stirred for 30 min to allow for hydration. Then, the solutions (inside capped bottles) were heated in a water bath under continuous stirring conditions. The heating regime differed for the two polymer types: 45 min at 95 °C for the agar, and 20 min at 60 °C for the gelatin. The solutions were subsequently poured into cylindrical syringes (diameter: 26 mm, volume: 65 mL; Omnifix, B. Braun); the syringes' interiors had been lightly coated with sunflower oil. The syringes were kept at 4 °C for 15–18 h to allow gelation to occur. Afterwards, the cylindrical gels were removed from the syringe using the plunger and cut into 5-mm-thick cylinders using a custom-built cutting frame. The gels were then assembled by stacking two individual cylinders. The two stacked layers were not glued with any external adhesive agent. Combinations were created with cylinders that differed in polymer type and fracture stress (Fig. 1b). To improve the echogenic properties of the interface between the two layers, the top of the lower layer was dusted with a small quantity (<10 mg) of agar powder prior to the placement of the upper layer. Preliminary experiments confirmed that the powder did not have any effects on the mechanical properties of the stacked gels.

2.2. Preparation of the artificial tongue model

The ATM employed in this study was also used in Srivastava et al. (2021). To describe the preparation method briefly, a polyvinyl alcohol

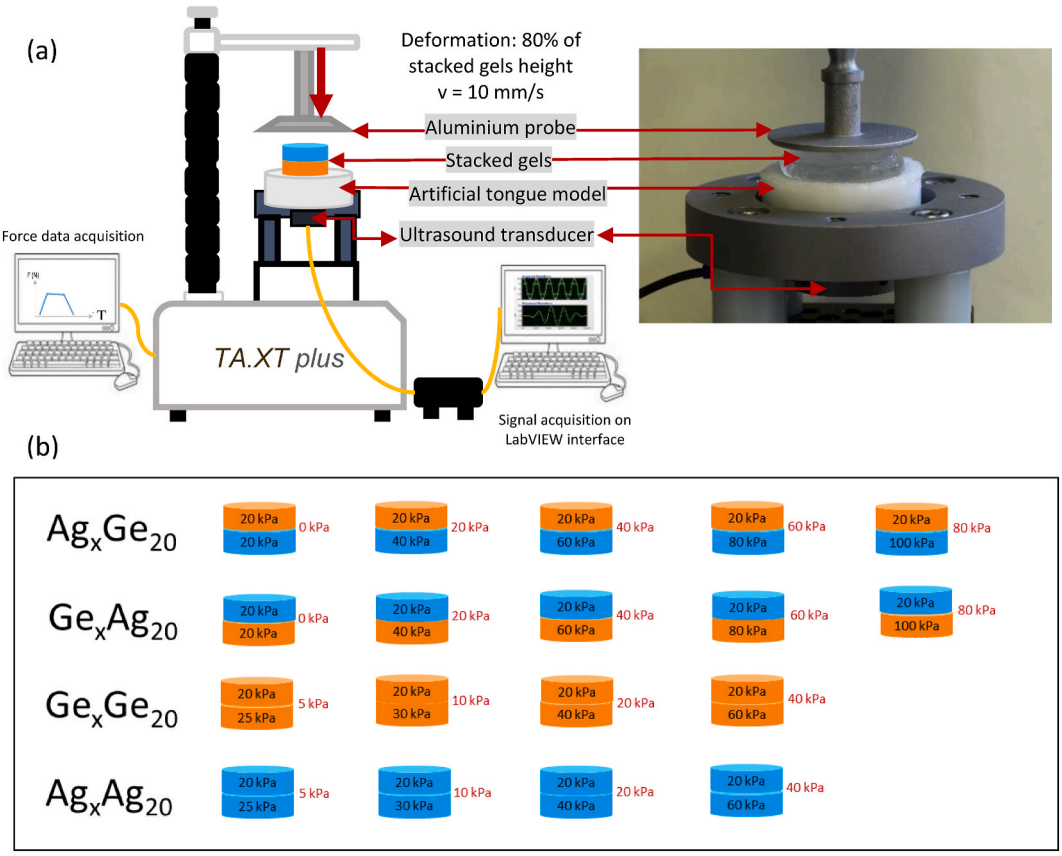

Fig. 1. (a) Schematic representation of the experimental set-up; (b) the combinations of stacked gels tested (including the flipped combinations).

solution (PVA; Sigma Aldrich, Saint-Louis, USA) was made using ultra-pure water (10% w/w); it then underwent stirring at 80 °C for 2 h. The solution was subsequently cooled to 20 °C and poured into a cylindrical mold made of polyvinyl chloride (diameter: 50 mm, height: 20 mm); at the bottom of the mold was P40 sandpaper (grain size: 425 μm; Norton, Saint-Gobain, France). The sandpaper was used to create a topological surface profile similar to that of a human tongue. After being carefully sealed, the mold and its contents were frozen (−20 °C for 10 h) and subsequently thawed (20 °C for 14 h). A total of six freezing-thawing cycles were performed to obtain the proper rigidity for a PVA hydrogel (Fromageau et al., 2007). Finally, the ATM was unmolded and stored in reverse osmosis treated water at room temperature (20 °C). This PVA based ATM can be stored at room temperature without any deterioration and any modification of mechanical properties for several months.

Young's modulus and surface roughness values for the ATM had been previously characterized using a texture analyzer and a contact profilometer, respectively (Srivastava et al., 2021). The Young's modulus value was 71 ± 2 kPa. Ishihara et al. (2013) found that the rigidity values of the human tongue at rest and in a contracted state were 12.2 ± 4.2 kPa and 122.5 ± 58.5 kPa, respectively. Surface roughness profile in terms average peak height (R_a) and correlation length (peak width, β) was 103 ± 3 μm and 429 ± 63 μm respectively. For the human tongue, average peak height appears to be 42.5–101.4 μm (Uemori et al., 2012), while peak width appears to be 355–878 μm (Andablo-Reyes et al., 2020).

2.3. Test sequence and ultrasound measurements

The ultrasonic analysis equipment and measurement principles are very similar to what was done in our previous studies, in which the analysis technique and procedure are also described in detail (Mantelet et al., 2020a,b; Srivastava et al., 2021). The main changes are the choice of a higher frequency ultrasound transducer, the use of a US pulser-receiver with a higher pulse recurrence frequency, and the development of a new image processing method for the analysis of the different interfaces. All these new elements are described in detail in the following lines.

The experimental set-up (Fig. 1a) included a texture analyzer, an ATM and a 5 MH mono-element piezoelectric ultrasound transducer (Olympus, Shinjuku, Tokyo, Japan) placed in contact (underneath) with the ATM. The use of a 5-MHz ultrasound frequency resulted in improved spatial resolution compared to previous work (maximum ultrasound frequency of 1 MHz; Mantelet et al., 2020a and b), which was crucial for performing measurements at the tight interface between the two layers. The transducer was connected to an ultrasound pulser-receiver (Ultrasound-Key, Lecoeur Electronique, Chuelles, France), which produced a negative square pulse wave signal (width setting: 24/255, amplitude: 100 V). The transducer digitized the radio frequency (*rf*) signals corresponding to the pulse-echo response of the system (quantification: 12 bits, sampling rate: 80 MHz, gain: 20 dB). The acquisition of the rf signals was done in real time during the tests using a dedicated user interface developed with LabVIEW® (LabVIEW, National Instruments, Austin, Texas, USA). The pulse recurrence frequency was approximately 450 Hz. This level was significantly higher than that used in previous research (maximum of 90 Hz; Mantelet et al., 2020a and b), allowing for better temporal resolution during the fast processes taking place. As a result, it was possible to conduct more detailed analyses of the signal fluctuations associated with the mechanical phenomena occurring at the interface between layers.

Before beginning the compression test, any water on the ATM's surface was carefully removed using absorbent paper (Kimtech™, Kimberly-Clark, Irving, TX, USA). A stacked gel combination was then gently placed on the ATM. The circular aluminum probe (diameter: 40 mm) of the texture analyzer was used to apply uniaxial stress to the gel-

ATM system. The amplitude of the probe displacement was 80% of the thickness of the stacked gels, subjecting the entire system (ATM [20 mm] and the two gel layers [5 mm each]) to compression, imposing a deformation rate of approximately 25% (when considering the ATM and the gel as a single entity). Compression speed was 10 mm/s, and the system was kept in a compressed state for 2.5 s before the probe was lifted. This holding step was necessary to examine relaxation phenomena. The probe is not lifted up during the latter stage.

During each test, the ultrasound measurements were performed in two steps. First, a reference signal was acquired by putting the transducer in contact with the ATM prior to gel placement. Then, ultrasound signals were acquired in real time (approximately 450 signals per second) during the test sequence, which began 0.5 s before compression was initiated and was followed by the 2.5-s holding step. It is also important to highlight that the ultrasonic system has negligible thermal effects due to the low intensity and short duration of the pulses.

2.4. Signal analysis

High-frequency noise reduction with a low-pass filter (cut-off frequency: 8 MHz) was applied to the fast Fourier transforms (FFTs) of all the *rf* signals. Fig. 2a and c shows a motion-mode (M-mode) image of the modulus of the Hilbert transform of all the signals acquired over the course of two tests, viz. $Ag_{20}Ge_{40}$ and $Ge_{20}Ge_{40}$ respectively. M-mode images depict changes in ultrasound signals over time. The x-axis corresponds to the time elapsed during a test. The y-axis corresponds to the time elapsed after each ultrasonic signal has been emitted. At a rate of approximately 450 *rf* signals were emitted per second. In Fig. 2a and c, there are three yellow traces—each corresponds to an echo generated by an ultrasound wave meeting an interface. E_0 corresponds to the acoustic energy reflected from the interface between the ATM and the lower gel layer (layer #1). E_1 is the response for the interface between the lower and upper gel layers (layers #1 and #2). E_2 is the response for the interface between the upper food layer and the probe. During a test sequence, all the echoes evolved, both in terms of amplitude (peak height) and of ToF (peak time of occurrence).

In the first phase of signal processing, an analysis was performed of ToF_E_0, the time of flight of the echo E_0. The ToF calculation determined the first zero-crossing (i.e., the time point where the sign of *rf* signal amplitude changes) after the signal amplitude had exceeded a threshold equal to twice the level of noise. This process yielded ToF_E_0(t) for the entire experimental test (Fig. 2b and d).

In the second phase of signal processing, an analysis was performed of the ToF of the echoes E_1 and E_2 (ToF_E_1 and ToF_E_2, respectively). Semi-automatic procedures were developed to perform this analysis due to the complexity of the ultrasound signals that followed echo E_0 (multiple reflections, overlapping signals, highly variable amplitude). First, the M-mode image for the entire trial was plotted. The modulus of

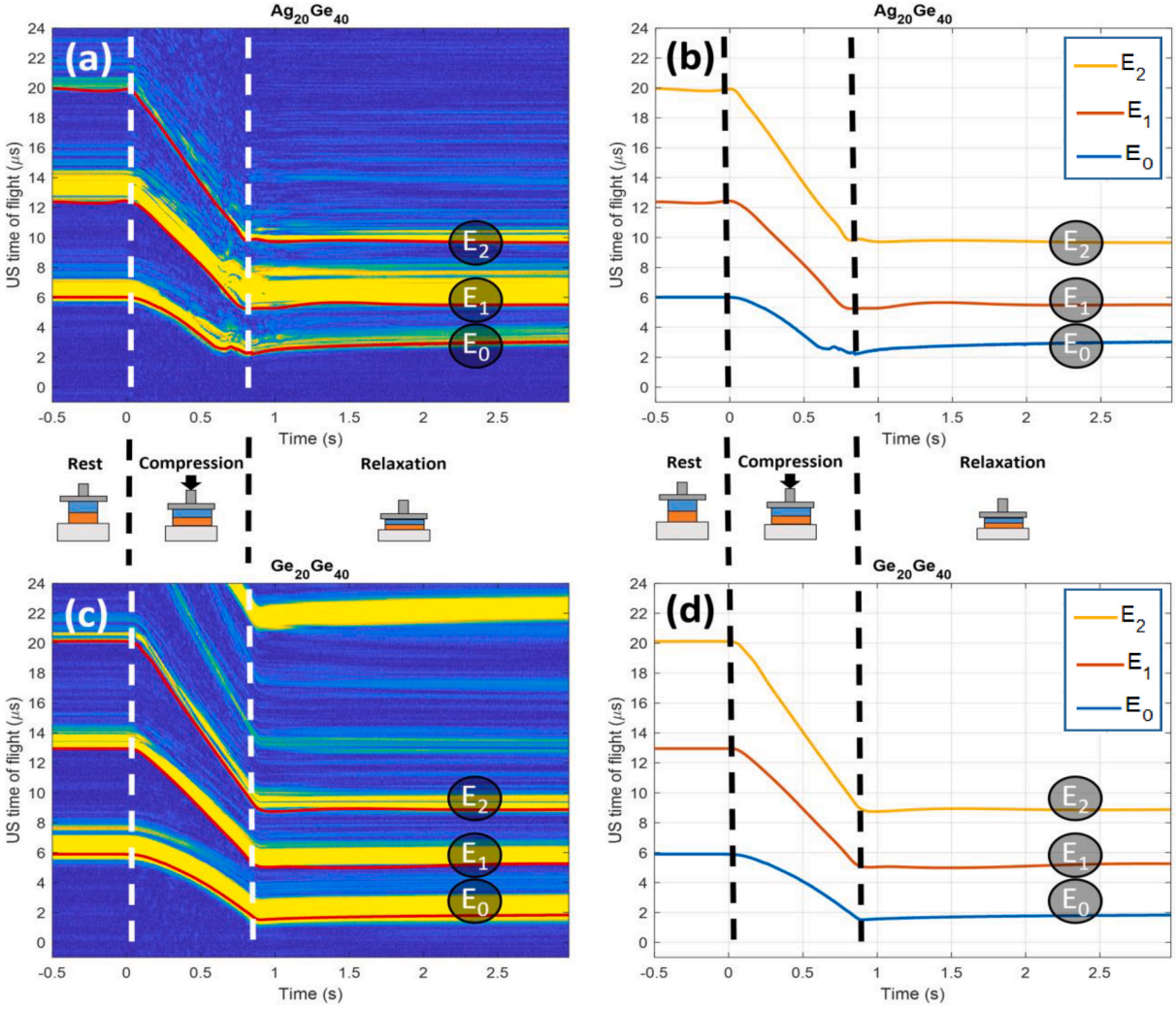

Fig. 2. Ultrasound M-mode image, where the x-axis is the time elapsed during a given test and the y-axis is the time delay between ultrasound emission and echo detection by the transducer (a: $Ag_{20}Ge_{40}$ and c: $Ge_{20}Ge_{40}$); variation in time of flight for the E_0, E_1, and E_2 echoes during a test, obtained from the analysis of the M-mode image and the corresponding *rf* signals (b: $Ag_{20}Ge_{40}$ and d: $Ge_{20}Ge_{40}$).

the Hilbert transform of the signals was used (as in Fig. 2a and c). As mentioned above, such plots allow all the echoes from an experimental trial to be clearly visualized. Next, a set of points in the profiles of E_1 and E_2 was manually selected. Due to the duration of the ultrasound pulse, the yellow traces corresponding to each echo had a specific width in the M-mode image (see Fig. 2a and c). When selecting the points, the idea was to follow the changes in each echo over time, moving from the blue zone (before the echo occurred) to the yellow zone (at the beginning of the echo). This method allowed ToF values to be selected in relation to the first zero-crossing event. Then, a MATLAB program employing an interpolation function (Spline method: cubic interpolation of values at neighboring points) was utilized to generate the full profiles of changes in ToF for each echo over the course of the experimental trial (ToF_E_1 [t] and ToF_E_2 [t] for E_1 and E_2, respectively; Fig. 2b and d).

2.5. Data processing

Signal processing yielded ToF data for the echoes originating from the three interfaces: ToF_E_0(t), ToF_E_1(t), and ToF_E_2(t). During a given test, there were three time points of interest—t_0, t_1, and t_2—that corresponded to the moment before compression, the end of compression step, and the end of 2.5 s holding step, respectively. During each test, the change in ToF for each echo depended on two main parameters. The first parameter was the propagation speed of the ultrasound waves, which was similar for the ATM, agar gel, and gelatin gel (~1500 m/s). It varied a negligible amount during compression, as it is governed above all by media compressibility and density (which were highly similar in this study). The second parameter was the path length of the ultrasound wave. The greater the length, the longer the flight time. In the experimental tests, the path length of the wave within one of the layers (ATM, agar gel, or gelatin gel) was twice as long as layer thickness. The deformation of each system component can thus be estimated as follows:

ATM deformation in millimeters (Δl_T):

$$\Delta l_T(t) = \frac{1500}{2}\left(TOF_{E0}(t) - TOF\_E_0(t_0)\right) \quad (1)$$

Layer 1 deformation in millimeters (Δl_{L1}):

$$\Delta l_{L1}(t) = \frac{1500}{2}\left(TOF_{E1}(t) - TOF\_E_1(t_0)\right) - \Delta l\varepsilon_T(t) \quad (2)$$

Layer 2 deformation in millimeters (Δl_{L2}):

$$\Delta l_{L2}(t) = \frac{1500}{2}\left(TOF_{E2}(t) - TOF\_E_2(t_0)\right) - \Delta l_{L1}(t) \quad (3)$$

This should be noted that the radius of the ultrasound beam (around 10 mm) is less than that of the gel layer. Hence the obtained values by above equations only indicates deformations observed at very central part of ATM-gel interface.

The resulting values of Δl_T, Δl_{L1}, and Δl_{L2} thus convey the real-time changes in thickness for each component. Another approach is to express these values relative to the global deformation applied to the system (which also corresponds to the amplitude of probe displacement). These percentages can be used to analyze the relative deformation experienced by each system component:

$$\varepsilon_T(t) = 100^* \frac{\Delta l_T(t)}{\Delta l_T(t) + \Delta l_{L1}(t) + \Delta l_{L2}(t)} \quad (4)$$

$$\varepsilon_{L1}(t) = 100^* \frac{\Delta l_{L1}(t)}{\Delta l_T(t) + \Delta l_{L1}(t) + \Delta l_{L2}(t)} \quad (5)$$

$$\varepsilon_{L2}(t) = 100^* \frac{\Delta l_{L2}(t)}{\Delta l_T(t) + \Delta l_{L1}(t) + \Delta l_{L2}(t)} \quad (6)$$

It is important to note that these indicators do not correspond to the deformation endured by the layers in relation to their initial thickness. It is important to note that these indicators do not correspond to the deformation endured by the layers in relation to their initial thickness.

In this study, the obtained results of deformations (for a set of at least seven repetitions) are presented and analyzed in different ways. Some parameters (force and ATM deformation) are studied by a temporal evolution throughout a test. For those, a graphical representation in the form of an average curve and an envelope corresponding to the standard deviation was chosen. This type of representation allows discussion of several conditions on the same graph. And, to conclude on the significance of differences, the envelopes around the curves were taken into account.

The second type of data (distribution of deformation in the individual layers) representation and analysis is done at given time spots (t_0, t_1 and t_2) during a test. For this, a representation in the form of histograms was used where each bar corresponds to a mean value, and the error bar to a standard deviation. Here, an ANOVA test was performed using XLSTAT (Addinsoft, Paris, France) with a complimentary post hoc analysis (Tukey HSD) test.

3. Results and discussion

The different stacked gels considered in the present study are summarized in Table 1 along with information on the observation of the fracture within each monolayer layer during the tests. The mechanical properties of all the monolayer gels used in this study (to build different combinations) had been previously characterized by Santagiuliana et al. (2018) — these values of Young's modulus and fracture stress are republished here in Table 2. [The formulation of the gels were done strictly as in aforesaid study to obtain the same mechanical values.] However, for fracture strain of each monolayer, the values reported in the aforesaid publication have here been converted to be expressed as a percentage of total displacement of the probe during our acoustical experiments, where a total deformation of 8 mm was applied on the system comprising three components (30 mm thick): a ATM (20 mm thick) and two layers of food gels (each 5 mm thick). The values of fracture strain described in the table thus correspond to the proportion of the total displacement of the plate from which the fracture of a 5 mm thick gel is expected. This was done to facilitate easier discussion with the parameters ε_{L1} and ε_{L2}. It can be noted that the agar and gelatin monolayer gels have distinctly different fracture strains but within themselves they didn't vary greatly (agar: 21.0–23.4% and gelatin: 39.3–46.9%). The differences in the obtained fracture strain between gelatin and agar gels is primarily due to the polymer type and resulting gel microstructure. Ikeda, Sangu and Nishinari (2003) have shown that agar gels show lower fracture strain values when compared to gelatin. Also the study further reports that with increase in polymer concentration gelatin based gels have shown increments in fracture strain while a slight decrease was seen for agar based gels. Finally, with regard to Young's modulus, it can be seen that agar monolayer gels had much varied values than gelatin gels (agar: 11.3–125.8 kPa and gelatin: 8.0–40.7 kPa).

In this section, first we discuss the impact of the overall mechanical properties of the gels on the ultrasound-assisted measurement of ATM

Table 1
Tabular representation of the different combinations of gel layers selected to form the stacked gels considered in the present study (in white). The presence of the letter "F" in a box indicates that the corresponding layer fractured during the experiments (confirmed both by visual inspection of the gels after the tests and by the presence of sudden drops in the ultrasound traces).

	Ag_{20}	Ag_{25}	Ag_{30}	Ag_{40}	Ag_{60}	Ag_{80}	Ag_{100}	Ge_{20}	Ge_{25}	Ge_{30}	Ge_{40}	Ge_{60}	Ge_{80}	Ge_{100}
Ag_{20}		F F	F F	F	F			F			F	F	F	F
Ge_{20}	F			F										

F Fractured Not fractured Not tested

Table 2
Mechanical characteristics—Young's modulus, fracture stress, and fracture strain values—of different individual gels (reproduced from Santagiuliana et al., 2018). The means and standard deviations (SD) are indicated. Threshold fracture strain (%) was calculated with respect to the total deformation of the food-tongue system (percentage of the total amplitude of probe displacement [8 mm] at which a 5-mm-thick gel is expected to fracture).

Gel	Polymer concentration (w/w in water)	Young's modulus (kPa)		Fracture stress (kPa)		Fracture strain (%)	
		Mean	SD	Mean	SD	Mean	SD
Ag_{20}	0.81	11.3	1.7	19.7	1.2	21.0	1.2
Ag_{25}	0.94	14.2	3.3	24.7	1	21.4	1.2
Ag_{30}	1.06	18.7	2.7	30.6	1	22.6	1.2
Ag_{40}	1.31	24.7	6	39.8	2	23.4	1.2
Ag_{60}	1.81	48.3	8	62.1	2.7	23.4	1.2
Ag_{80}	2.31	67.1	20.5	79.6	3.5	23.4	1.8
Ag_{100}	2.80	125.8	12	102.1	3.2	23.0	0.6
Ge_{20}	4.03	8	1.6	20.5	2.5	39.3	4.8
Ge_{25}	4.54	10.3	2.1	25.2	1.3	39.5	3.0
Ge_{30}	5.05	11.7	2	31.3	2.7	40.8	5.4
Ge_{40}	6.07	18.5	4.3	40.9	2.7	42.1	4.8
Ge_{60}	8.11	24	3.2	60.7	3.5	43.7	5.4
Ge_{80}	10.15	33.3	5.2	78.8	3.3	44.6	4.2
Ge_{100}	12.19	40.7	4.3	103.4	3.7	46.9	7.1

deformations. Then, the focus is placed on characterization of the individual behaviors of the different layers composing the stacked gels. In each of these two parts, we will thus be able to better understand the impact of different parameters on the mechanical behavior of stacked gels subjected to compression and then to relaxation, between a deformable ATM and a hard plate. These behaviors will be studied by considering several factors: impact of the type of polymer association, the polymer content of the gels, or the orientation of the gels (surface in contact with the ATM). It is important to recall that, in the study's experimental set-up, the diameter of the ultrasound beam (less than 10 mm) was smaller than the diameter of the gels (26 mm prior to compression).

3.1. *Impact of gel properties on the deformation of the artificial tongue model*

First, the effect of gels properties on ATM deformation was examined. The ultrasound measurements made it possible to correlate the degree of deformation with the force measured by the texture analyzer. This relationship is important because, in real life, tongue deformation during food oral processing could directly impact mechanoreceptor stimulation. In particular, two experimental situations were considered: tests in which a Ge_{20} layer was coupled with a variety of gelatin layers (Ge_{25}, Ge_{30}, Ge_{40}, and Ge_{60}; Fig. 3a and b) and tests in which an Ag_{20} layer was coupled with a variety of agar layers (Ag_{25}, Ag_{30}, Ag_{40}, and Ag_{60}; Fig. 3c and d). Fig. 3a presents the variation of force exerted during the compression of stacked gels both composed of gelatin, with top layer as Ge_{20}, combined with bottom layers with varied fracture stresses (Ge_{25}, Ge_{30}, Ge_{40}, Ge_{60}). The envelopes around bold colored lines represent standard deviation obtained over seven repetitions. Fig. 3b

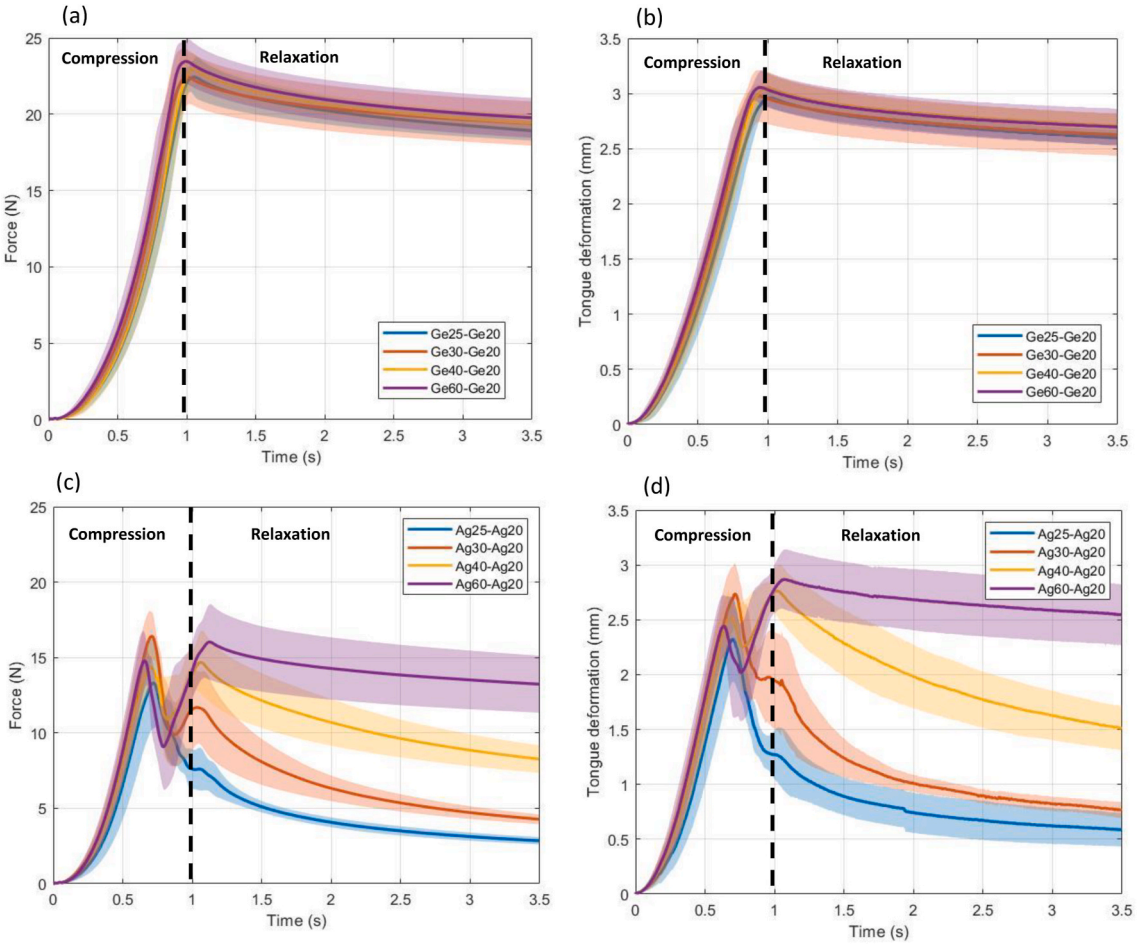

Fig. 3. (a) Force and (b) deformation experienced by the ATM during the compression of stacked gels in which a Ge_{20} layer was paired with another gelatin layer (Ge_{25}, Ge_{30}, Ge_{40}, or Ge_{60}); (c) force and (d) deformation experienced by the ATM during the compression of stacked gels in which an Ag_{20} layer was paired with another agar layer (Ag_{25}, Ag_{30}, Ag_{40}, or Ag_{60}). The envelopes around the thick colored lines show the standard deviations obtained from seven replicates.

represents, for the same gels, the evolution of the ATM deformation over the course of compression. It can be observed from the figures that the variation of estimated ATM deformation was in accordance with that of force, which is congruent with the observation from our previous results (Srivastava et al., 2021). However, varying the fracture stress of the lower gelatin layers paired with Ge_{20} had no significant impact (overlapping standard deviation envelopes), neither at the end of compression step or during relaxation.

In the second situation, where Ag_{20} served as the upper layer and the second agar layer was on bottom (Fig. 3c and d), varied responses were obtained. During compression (between 0 and 1 s), the sudden drop in force signaled that at least one of the gel layers had fractured. The results also indicate that ATM deformation varied markedly during the relaxation. In real life, such phenomena could contribute to perceived heterogeneity and should hence be studied further. At the end of 2.5 s holding step, different stacked gels displayed greatly contrasting force and deformation profiles. The higher the agar concentration in the lower layer (i.e., the higher the fracture stress), the smaller the decrease in the force and deformation experienced by the ATM. In all cases, the upper Ag_{20} layer fractured (Table 1); however, lower layers when composed of Ag_{40} and Ag_{60} did not. Consequently, comparing the results for the gelatin and agar gels, the brittle nature of agar might explain the drastic variation in force and deformation that was observed. Furthermore, the sudden appearance of variation in deformation was consistent with the visual signs of fracture in the samples at the end of the tests (Table 1).

For all the gel combinations used in the study, an analysis was performed of force patterns at the end of compression step (t_1) and holding step (t_2) (Fig. 4a); ATM deformation at these two time points was also examined (Fig. 4b). Measurements were organized into four different groups based on the four biopolymer combinations studied. In both figures, a dotted line indicates where force and deformation were identical at times t_1 and t_2. Thus, when a point is closer to this line (i.e., "no relaxation"), it indicates that there was less change in the force and deformation experienced by the ATM during relaxation. Conversely, when a point is closer to the x-axis (i.e., "high relaxation"), it indicates that the force and deformation experienced by the ATM decreased during relaxation. The results highlight the similarities in the distribution of points within the different groups (Fig. 4a and b).

When Ag_{20} or Ge_{20} were paired with different gelatin layers, profiles of force and deformation for the ATM were fairly similar across gels combinations (especially when both layers were gelatin based) (Fig. 4a and b; orange and purple points). This finding can be explained by the fact that gelatin gels are more elastic. When the stacked gels were entirely composed of gelatin, the measurement points clustered together, suggesting a consistent response despite the differences in Young's modulus values. They displayed a low degree of relaxation behavior, given that they remained close to the "no relaxation" line. The reason behind the low relaxation in gelatin based gels could be due its

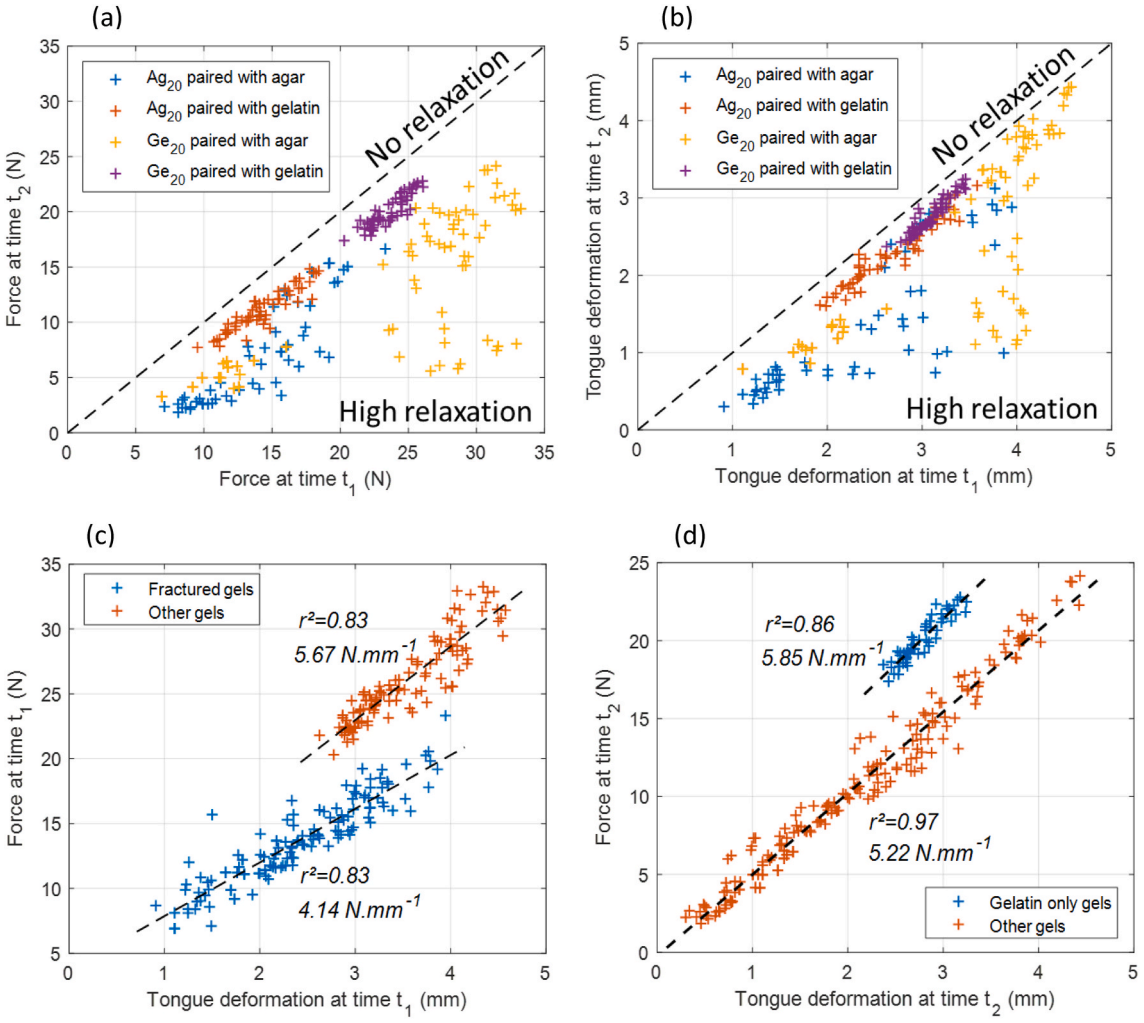

Fig. 4. (a) Force experienced by the ATM at the end of holding step (t_2) versus at the end of compression step (t_1); (b) deformation experienced by the ATM at the end of holding step (t_2) versus at the end of compression step (t_1); (c) force versus deformation at the end of compression step (t_1); (d) force versus deformation at the end of holding step (t_2).

prominent strain hardening behavior at higher deformation.

However, when a layer composed of Ag_{20} or Ge_{20} was paired with different layers of agar, there was greater variability in these profiles at the end of compression step, and, comparatively, a higher degree of relaxation was observed (Fig. 4a and b; blue and yellow points). The measurement points were more scattered because of the higher fracture behaviors reported in the agar-agar combinations due to higher stress concentration. Moreover, few of the agar layers also fractured even when paired with a gelatin layer (Table 1).

Although the force and deformation experienced by the ATM was generally consistent across groups (Fig. 4a and b), slight differences were observed. For example, the two point clusters (blue and yellow) corresponding to stacked gels with an Ag_{20} or Ge_{20} layer paired with agar layers displayed distinct force values (Fig. 4a); there was some overlap, however, in deformation values (Fig. 4b). Moreover, when Ge_{20} was paired with agar, some of the data points in the high range of deformation at time t_1 (between 3.5 and 5 mm) exhibited low relaxation behavior in terms of ATM deformation (remaining close to the dotted line) which could not be confirmed on the force plots.

The next step was to compare the force and deformation experienced by the ATM at the end of compression step (t_1) and holding step (t_2) (Fig. 4c and d, respectively). Two distinct clusters of points can be seen; each seems to form a straight line. It appears that the clusters correspond to, respectively, the stacked gels in which compression caused at least partial fracturing ($r^2 = 0.83$) versus no fracturing ($r^2 = 0.83$) (Fig. 4c). Cluster composition however differed at time t_2 (Fig. 4d). One cluster consisted of the 100% gelatin stacked gels ($r^2 = 0.86$), while the other consisted of all the other combinations, meaning gels with at least one agar layer ($r^2 = 0.97$).

In Fig. 4c, for the same level of deformation, it can be seen that, at the end of compression step, higher levels of force were associated with gels that had not fractured. One possible explanation for the observed differences is that the surface upon which the force was exerted was not the same. Consequently, for a given level of deformation, the higher force values could have been associated with larger contact surfaces. The differences in surface characteristics between the ATM and the gel could explain these different behaviors. During compression, adhesion and friction between the bottom-layer gel and the ATM may have acted in an opposing manner to the increase in contact area (i.e., a barreling effect; Brennan and Bourne, 1994; Pons and Fiszman, 1996). Under conditions of compression, a barreling effect can arise due to friction between a cylindrical sample and the plate below (in this study, an ATM), leading to triaxial instead of uniaxial stress. Experiencing deformation, the gel may thus have tended to bend even as the area in contact with the ATM remained the same. A similar pattern emerged at the end of holding step for the 100% gelatin stacked gels, as compared to the other gel combinations (Fig. 4d). The non-linear response of gelatin gels under high deformations (i.e. strain hardening) when compared to more linear response of agar gels until fracture (due to higher brittleness) could explain the higher force for gelatin only gels at relaxation step.

It is important to recall that, in the study's experimental set-up, the diameter of the ultrasound beam (less than 10 mm) was smaller than the diameter of the gels (26 mm prior to compression). Thus, the deformation measured by ultrasound only reflected what was happening in the central part of the ATM. To obtain information about radial ATM deformation, it would be necessary to use a multiple-element transducer (an array-type transducer, as employed in imaging). It would then be easier to observe any barreling effects.

The results discussed in this section underscore the utility of ultrasound methods, highlighting their complementarity with force measurement methods. The latter make it possible to study the mechanical responses of multi-layer heterogeneous materials, such as an ATM in contact with stacked gels differing in mechanical properties. However, the results also made it clear that a comprehensive mechanistic interpretation of our findings requires characterizing the phenomena that occurred within the stacked gels. The second part of the discussion focuses on this subject.

3.2. Distribution of deformation: the tongue-food system

This study makes a contribution to the field by describing an ultrasound method for investigating how the different components of a model tongue-food system experience deformation over time. Thanks to this methodology, it was clear that deformation dynamics varied across experimental situations (Fig. 5). First, results were analyzed for the stacked gels in which the upper layer was Ag_{20} and the lower layer was also an agar gel (Ag_{25}, Ag_{30}, Ag_{40}, or Ag_{60}); the deformation of the ATM (ε_T), lower layer (ε_{L1}), and upper layer (ε_{L2}) were examined relative to the total deformation experienced by the system. For example, under conditions of compression, 17% of the total deformation was shared by the ATM, 36% by the Ag_{25} gel, and 46% by the Ag_{20} gel (first bar in Fig. 5a).

Two other factors affected the results: layer position and the time at which the measurement was made (compression vs. relaxation) (Fig. 5). In one situation, Ag_{20} served as the upper layer (Fig. 5a and b), while in another situation, the sample was flipped, and Ag_{20} served as the lower layer (Fig. 5c and d). When Ag_{20} was on top, the system underwent compression (Fig. 5a: measurements at t_1) and relaxation (Fig. 5b: measurements at t_2). The same was true when Ag_{20} was on the bottom (Fig. 5c: measurements at t_1 and Fig. 5d: measurements at t_2).

When Ag_{20} served as the upper layer, it experienced high and consistent levels of deformation that were independent of the composition of the lower agar layer (Fig. 5a). These levels (46–48%) were much greater than the fracture threshold (21.0% on average; Table 2); this result was consistent with observed fracturing at the end of the tests and or when tracing the ToF profiles. As the concentration of agar in the lower layer climbed (Ag_{25}, Ag_{30}, Ag_{40}, and Ag_{60}), there was a clear trend in which the increase in Young's modulus values led to the decreased deformation of the lower agar layers and the increased deformation of the ATM (i.e., in compensation). The deformation levels of Ag_{25} and Ag_{30} were consistent with the visual signs of fracturing. Under conditions of relaxation (Fig. 5b), the Ag_{20} gel on top continued to undergo deformation, while the ATM returned to its initial state. A degree of compensation was provided by the fractured lower agar layer. Such was also true when Ag_{25} and Ag_{30} were used in the bottom layer—they continued to experience deformation during the relaxation stage. The same general trends were seen when the stacked gels were flipped and the Ag_{20} layer was found on bottom (Fig. 5c and d). Although the differences were not significant (based on the overlap in the standard deviations), the Ag_{20} layer tended to experience less deformation when it was on bottom. In contrast, the deformation of the upper layer became more pronounced. When the upper layer was composed of Ag_{40}, the level of deformation (40%) was much higher (Fig. 5d) than in all the other cases; it was also higher than the fracture threshold (23.4%; Table 2), suggesting that fracture was very likely to occur. These differences resulting from layer position could be explained by changes in surface interactions, namely whether gel layers were in contact with the ATM (composed of soft PVA) or with the palate-mimicking probe (composed of rigid aluminum). These interactions may promote or mitigate gel spreading over the course of compression or relaxation. In summary, the results demonstrate that the ultrasound method did a good job of describing the deformation dynamics of the system's individual parts. The fact that slight differences were also observed when the stacked gels were flipped upside down is encouraging because it reflects the method's ability to independently distinguish deformation in the independent layers.

An analysis was then performed of the deformation dynamics in situations where a Ge_{20} layer was coupled with different types of agar layers (Fig. 6). The experimental approach was the same as that described above. In one situation, the upper layer was composed of Ge_{20} (Fig. 6a and b), while in another situation, the sample was flipped, and the lower layer was composed of Ge_{20} (Fig. 6c and d). When Ge_{20} was on

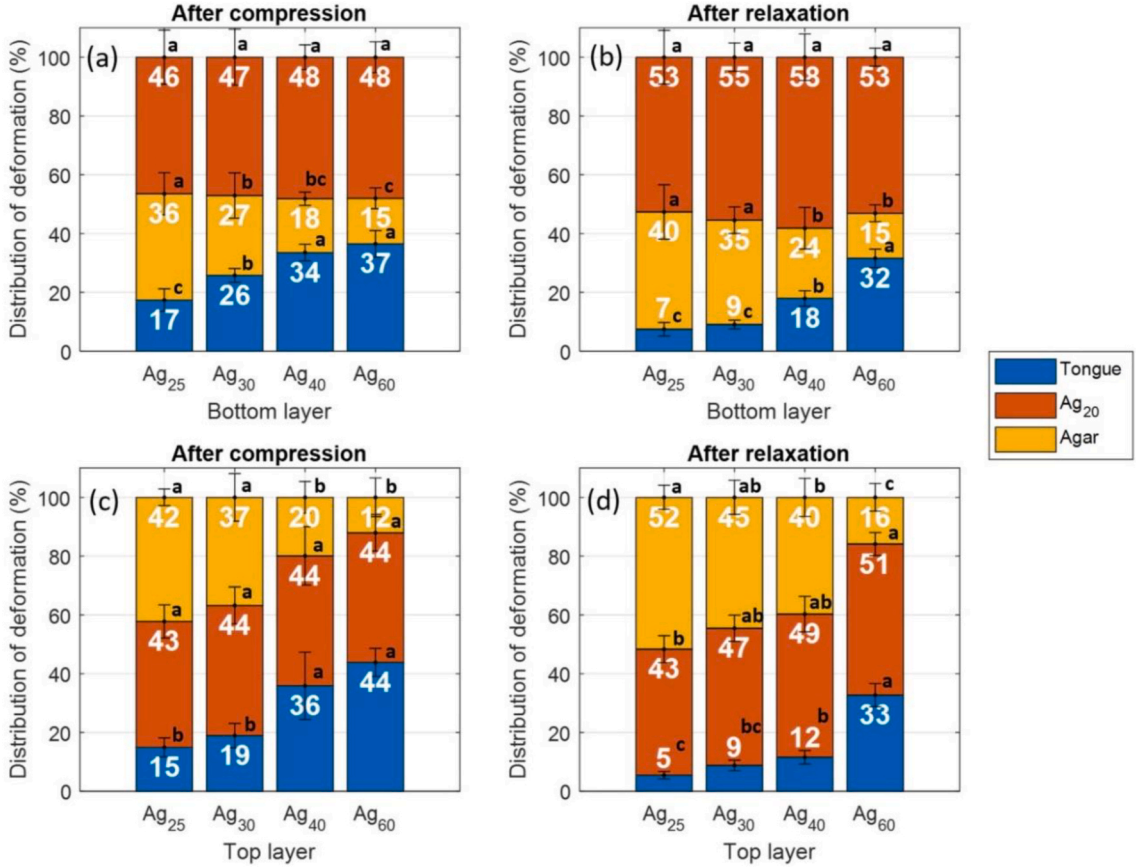

Fig. 5. Stacked bar graphs of the mean values and standard deviations of the relative deformation (%) undergone by the ATM (ε_T), lower gel layer (ε_{L1}), and upper gel layer (ε_{L2}), compared to total system deformation. Depicted here are the values for stacked gels in which an Ag_{20} layer was paired with another agar layer (Ag_{25}, Ag_{30}, Ag_{40}, or Ag_{60}). Ag_{20} was on top (layer L_2) in (a) and (b) and on bottom (layer L_1) in (c) and (d). Deformation at the end of compression step (t_1) is depicted in (a) and (c), and deformation at the end of holding step (t_2) is depicted in (b) and (d).

top, the system experienced compression (Fig. 6a: measurements at t_1) and relaxation (Fig. 6b: measurements at t_2). The same was true when Ge_{20} was on the bottom (Fig. 6c: measurements at t_1 and Fig. 6d: measurements at t_2). The average deformation values for the Ge_{20} layer ranged between 26 and 40%, remaining, in the vast majority of cases, below the fracture threshold (39.3%; Table 2). These measurements are thus consistent with the observation that the Ge_{20} layer was never fractured at the end of a test. Layer position generally had no effect on how the stacked gels responded to compression (Fig. 6a and c). However, the case in which a Ge_{20} layer was paired with an Ag_{20} layer was distinct. As noted above, the Ag_{20} layer experienced significant deformation (43–48%, above the fracture threshold). Conversely, when a Ge_{20} layer was paired with an agar layer composed of Ag_{40}, Ag_{60}, Ag_{80}, or Ag_{100}, the deformation of the agar gels was less pronounced and remained below the fracture threshold. Interestingly, even though these agar gels represented a wide range of Young's modulus values (24.7–125.8 kPa), they differed little in their deformation distributions. However, more marked differences appeared during relaxation (Fig. 6b and d). It should also be noted that these pronounced differences in the deformation of agar layer at t_1 and t_2 reflects the possibility of fracture to take place after the compression step. In particular, the deformation of the Ag40 layer exceeded the fracture threshold. Similarly, the deformation of the Ag_{60} layer tended to increase as well. As agar concentration climbed, moving from Ag_{20} to Ag_{100}, it was observed also that the deformation profile of the ATM changed significantly in the seconds following compression. Therefore, when the palate-mimicking probe was held in compression position, prominent mechanical phenomena (including fractures) occurred and could be monitored with ultrasound over response times longer than the duration of compression.

4. Conclusions

The ultrasound method described here was used to investigate how polymer type (agar or gelatin) affected the mechanical responses of stacked gels uniaxially compressed upon a biomimetic tongue. More specifically, the method made it possible to quantify the relative deformations of the individual components of the whole system: the artificial tongue model and the two gels layers. The degree of deformation was affected by polymer type (gelatin vs. agar), gel mechanical properties (degree of elasticity vs. brittleness), the specific combination of the two layers, and layer position (bottom vs. top). Changes in the gelatin concentration of the layers had no impact on their mechanical responses, while the opposite was true in the case of changes in agar concentration. This result most probably stems from the fact that gelatin is more elastic, while agar is more brittle.

In a real food oral processing context, the contribution of the ATM to the mechanical breakdown of this type of food is probably minor when compared to mastication. In this study, the compression of the gels by a flat probe (mimicking palate) also led to fracture of only a minority of gel types. The results, however, show that manipulation between the tongue and the palate can reveal a wide range of mechanical properties through the gels and may still greatly allow the texture to be assessed.

In summary, ultrasound methods show great promise for research seeking to investigate the mechanical behaviors of heterogeneous foods in contact with the tongue during oral processing. Beyond providing information about changes in the tongue's mechanical status over time, the methodology described here could be used to explore the mechanical phenomena that occur inside foods, which is impossible using traditional texture assessment techniques. Our future work will focus on

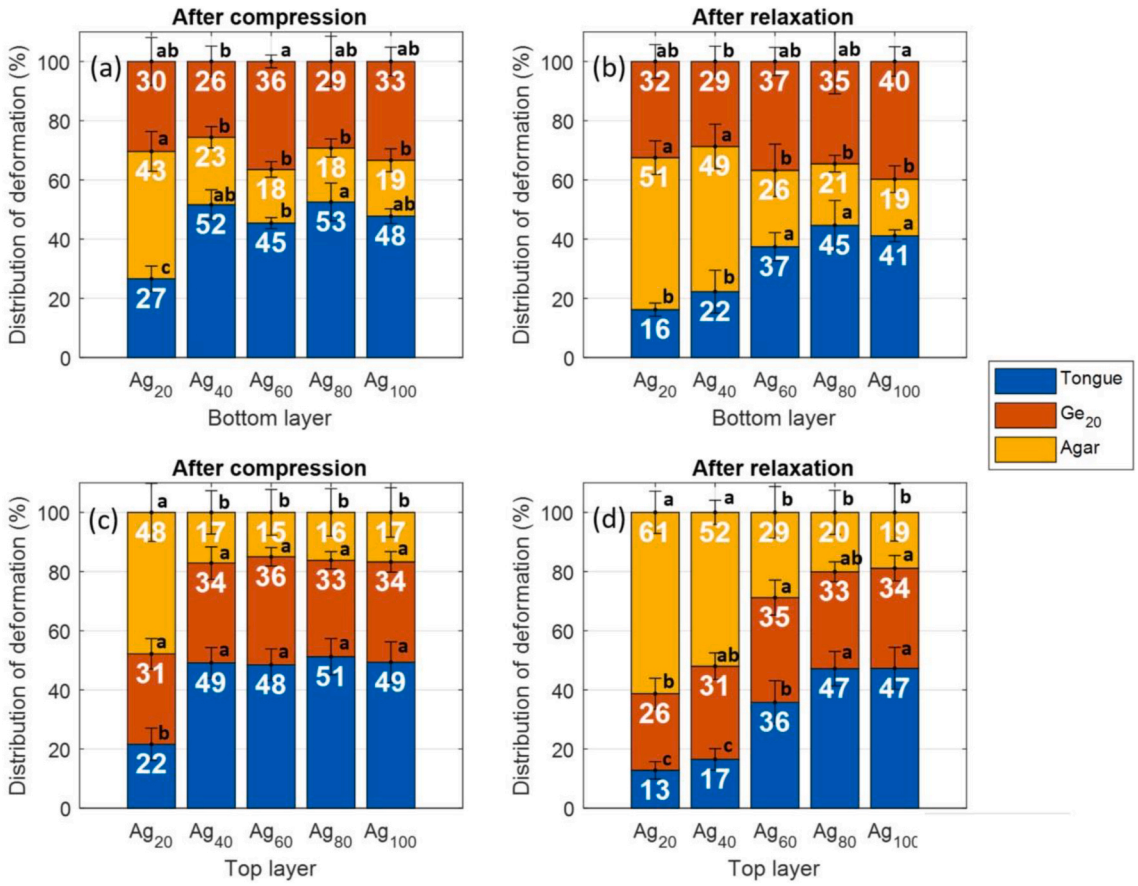

Fig. 6. Stacked bar graphs of the mean values and standard deviations of the relative deformation (%) undergone by the ATM (ε_T), lower gel layer (ε_{L1}), and upper gel layer (ε_{L2}), compared to total system deformation. Depicted here are the values for stacked gels in which a Ge_{20} layer was paired with an agar layer (Ag_{20}, Ag_{40}, Ag_{60}, Ag_{80}, or Ag_{100}). Ge_{20} was on top (layer L_2) in (a) and (b) and on bottom (layer L_1) in (c) and (d). Deformation at the end of compression step (t_1) is depicted in (a) and (c), and deformation at the end of holding step (t_2) is depicted in (b) and (d).

more complex foods with more local heterogeneities. Multi-element ultrasound probes and 2-D imaging could also help to trace volume changes in such artificial tongue models and foods, and to take us further towards monitoring more complex heterogeneities, as well as for detecting and localizing cracks that occur within the gels during fracture.

Funding

This work was financially supported by (i) the QUSToFood project funded by the French National Research Agency (ANR-17-CE21-004) and (ii) the international mobility grant (2018) awarded to Rohit Srivastava by the ABIES doctoral school (AgroParisTech – Université Paris-Saclay).

CRediT authorship contribution statement

Rohit Srivastava: Conceptualization, Methodology, Validation, Formal analysis, Investigation, Resources, Data curation, Writing – original draft, Writing – review & editing, Visualization, Supervision, Funding acquisition. **Markus Stieger:** Conceptualization, Methodology, Validation, Resources, Writing – review & editing, Supervision. **Elke Scholten:** Conceptualization, Methodology, Validation, Resources, Writing – review & editing, Supervision. **Isabelle Souchon:** Conceptualization, Methodology, Validation, Formal analysis, Resources, Writing – review & editing, Supervision, Project administration. **Vincent Mathieu:** Conceptualization, Methodology, Software, Validation, Formal analysis, Investigation, Resources, Data curation, Writing – review & editing, Visualization, Supervision, Project administration, Funding acquisition.

Declaration of competing interest

The authors declare that they have no known competing financial interests or personal relationships that could have appeared to influence the work reported in this paper

Acknowledgments

We thank Marco Santagiuliana for helping to design the model foods. We are grateful to Mary Ugwonali, David Forest, and Harry Baptist for their crucial technical support. We also thank Jessica Pearce-Duvet for proofreading this manuscript.

References

Andablo-Reyes, E., Bryant, M., Neville, A., Hyde, P., Sarkar, R., Francis, M., Sarkar, A., 2020. 3D biomimetic tongue-emulating surfaces for tribological applications. ACS Appl. Mater. Interfaces 12 (44), 49371–49385. https://doi.org/10.1021/acsami.0c12925.

Brennan, J.G., Bourne, M.C., 1994. Effect of lubrication on the compression behaviour of cheese and frankfurters. J. Texture Stud. 25 (2), 139–150.

Devezeaux de Lavergne, M.D., Tournier, C., Bertrand, D., Salles, C., Van de Velde, F., Stieger, M., 2016. Dynamic texture perception, oral processing behaviour and bolus properties of emulsion-filled gels with and without contrasting mechanical properties. Food Hydrocolloids 52, 648–660. https://doi.org/10.1016/j.foodhyd.2015.07.022.

De Wijk, R.A., Prinz, J.F., Janssen, A.M., 2006a. Explaining perceived oral texture of starch-based custard desserts from standard and novel instrumental tests. Food Hydrocolloids 20 (1), 24–34. https://doi.org/10.1016/j.foodhyd.2005.02.008.

De Wijk, R.A., Wulfert, F., Prinz, J.F., 2006b. Oral processing assessed by M-mode ultrasound imaging varies with food attribute. Physiol. Behav. 89 (1), 15–21. https://doi.org/10.1016/j.physbeh.2006.05.021.

Fromageau, J., Gennisson, J.L., Schmitt, C., Maurice, R.L., Mongrain, R., Cloutier, G., 2007. Estimation of polyvinyl alcohol cryogel mechanical properties with four ultrasound elastography methods and comparison with gold standard testings. IEEE Trans. Ultrason. Ferroelectrics Freq. Contr. 54 (3), 498–508. https://doi.org/10.1109/TUFFC.2007.273.

Ikeda, S., Sangu, T., Nishinari, K., 2003. Comparative studies on fracture characteristics of food gels subjected to uniaxial compression and torsion. Food Sci. Technol. Res. 9, 372e377. https://doi.org/10.3136/fstr.9.372.

Ishihara, S., Nakao, S., Nakauma, M., Funami, T., Hori, K., Ono, T., Kohyama, K., Nishinari, K., 2013. Compression test of food gels on artificial tongue and its comparison with human test. J. Texture Stud. 44 (2), 104–114. https://doi.org/10.1111/jtxs.12002.

Kohyama, K., Ishihara, S., Nakauma, M., Funami, T., 2019. Compression test of soft food gels using a soft machine with an artificial tongue. Foods 8 (6), 182. https://doi.org/10.3390/foods8060182.

Laguna, L., Sarkar, A., 2016. Influence of mixed gel structuring with different degrees of matrix inhomogeneity on oral residence time. Food Hydrocolloids 61, 286–299. https://doi.org/10.1016/j.foodhyd.2016.05.014.

Larsen, D.S., Tang, J., Ferguson, L., Morgenstern, M.P., James, B.J., 2016. Oral breakdown of texturally complex gel-based model food. J. Texture Stud. 47 (3), 169–180. https://doi.org/10.1111/jtxs.12146.

Le Bleis, F., Chaunier, L., Della Valle, G., Panouillé, M., Réguerre, A.L., 2013. Physical assessment of bread destructuration during chewing. Food Res. Int. 50 (1), 308–317. https://doi.org/10.1016/j.foodres.2012.10.042.

Mantelet, M., Restagno, F., Souchon, I., Mathieu, V., 2020a. Using ultrasound to characterize the tongue-food interface: an in vitro study examining the impact of surface roughness and lubrication. Ultrasonics 103 (April 2019), 106095. https://doi.org/10.1016/j.ultras.2020.106095.

Mantelet, M., Srivastava, R., Restagno, F., Souchon, I., Mathieu, V., 2020b. Real time ultrasound assessment of contact progress between food gels and tongue mimicking surfaces during a compression. Food Hydrocolloids, 106099. https://doi.org/10.1016/j.foodhyd.2020.106099.

Mesurolle, J., Saint-Eve, A., Déléris, I., Souchon, I., 2013. Impact of fruit piece structure in yogurts on the dynamics of aroma release and sensory perception. Molecules 18 (5), 6035–6056. https://doi.org/10.3390/molecules18056035.

Palczak, J., Giboreau, A., Rogeaux, M., Delarue, J., 2020. How do pastry and culinary chefs design sensory complexity? International Journal of Gastronomy and Food Science 19 (November 2019), 100182. https://doi.org/10.1016/j.ijgfs.2019.100182.

Pons, M., Fiszman, S.M., 1996. Instrumental texture profile analysis with particular reference to gelled systems. J. Texture Stud. 27 (6), 597–624. https://doi.org/10.1111/j.1745-4603.1996.tb00996.x.

Saint-Eve, A., Panouillé, M., Capitaine, C., Déléris, I., Souchon, I., 2015. Dynamic aspects of texture perception during cheese consumption and relationship with bolus properties. Food Hydrocolloids 46, 144–152. https://doi.org/10.1016/j.foodhyd.2014.12.015.

Salles, C., Kerjean, J.R., Veiseth-Kent, E., Stieger, M., Wilde, P., Cotillon, C., 2017. The TeRiFiQ project: combining technologies to achieve significant binary reductions in sodium, fat and sugar content in everyday foods whilst optimising their nutritional quality. Nutr. Bull. 42 (4), 361–368. https://doi.org/10.1111/nbu.12297.

Santagiuliana, M., Bhaskaran, V., Scholten, E., Piqueras-Fiszman, B., Stieger, M., 2019. Don't judge new foods by their appearance! How visual and oral sensory cues affect sensory perception and liking of novel, heterogeneous foods. Food Qual. Prefer. 77 (February 2019), 64–77. https://doi.org/10.1016/j.foodqual.2019.05.005.

Santagiuliana, M., Piqueras-Fiszman, B., van der Linden, E., Stieger, M., Scholten, E., 2018. Mechanical properties affect detectability of perceived texture contrast in heterogeneous food gels. Food Hydrocolloids 80, 254–263. https://doi.org/10.1016/j.foodhyd.2018.02.022.

Singh, H., Ye, A., Ferrua, M.J., 2015. Aspects of food structures in the digestive tract. Current Opinion in Food Science 3, 85–93. https://doi.org/10.1016/j.cofs.2015.06.007.

Srivastava, R., Mantelet, M., Saint-Eve, A., Gennisson, J.L., Restagno, F., Souchon, I., Mathieu, V., 2021. Ultrasound monitoring of a deformable tongue-food gel system during uniaxial compression-an in vitro study. Innovat. Food Sci. Emerg. Technol. 70, 102695. https://doi.org/10.1016/j.ifset.2021.102695.

Szczesniak, A.S., Kahn, E.L., 1984. Texture contrasts and combinations: a valued consumer attribute. J. Texture Stud. 15 (3), 285–301. https://doi.org/10.1111/j.1745-4603.1984.tb00385.x.

Uemori, N., Kakinoki, Y., Karaki, J., Kakigawa, H., 2012. New method for determining surface roughness of tongue. Gerodontology 29 (2), 90–95. https://doi.org/10.1111/j.1741-2358.2011.00509.x.

Young, A.K., Cheong, J.N., Hedderley, D.I., Morgenstern, M.P., James, B.J., 2013. Understanding the link between bolus properties and perceived texture. J. Texture Stud. 44 (5), 376–386. https://doi.org/10.1111/jtxs.12025.